AIAA JOURNAL
Vol. 47, No. 3, March 2009

Evidence of Nonlogarithmic Behavior of Turbulent Channel and Pipe Flow

Matthias H. Buschmann*
Institut für Luft- und Kältetechnik Dresden, 01309 Dresden, Germany
and
Mohamed Gad-el-Hak†
Virginia Commonwealth University, Richmond, Virginia 23284-3015

DOI: 10.2514/1.37032

Employing data of peak position and peak values of Reynolds shear stress provided by canonical channel flow direct numerical simulations and pipe and channel flow experiments, three recent theories predicting the mean-velocity profile of wall-bounded turbulent flows are compared. Based on that analysis it is verified that the mean-velocity profile of such internal flows is logarithmic only to leading order and that the higher-order terms are proportional to reciprocal powers of the Kármán number. This finding clearly indicates that higher-order effects with respect to the Kármán number and the wall-normal coordinate must be considered. Furthermore, our results show that even the statistics of the flow region closest to the wall are affected by flow phenomena that scale with outer variables.

I. Introduction

THE universal logarithmic law describing the mean-velocity profile in the overlap region of a turbulent wall-bounded flow is a cornerstone of fluid mechanics research. However, there is no physical or mathematical reason to exclude, a priori, a Reynolds number dependence of such profile. In fact, there has been considerable controversy during the past few years concerning the validity of the log law and alternative Reynolds-number-dependent power as well as logarithmic laws have been proposed (for references and background, see Buschmann and Gad-el-Hak [1]). Although a useful workhorse for engineering applications because of its simplicity, failure of the universal logarithmic law makes it more difficult to extrapolate laboratory-scale experiments and flow control devices to field conditions, as well as to calibrate a variety of wall sensors whose utility depends on the precision of the law of the wall. More seriously, if the classical law of the wall would fail, all recent numerical schemes based in one way or another on the logarithmic law would fail too (Gad-el-Hak [2]). Recent high-Reynolds-number experiments, direct numerical simulations (DNS), and theoretical considerations have strongly suggested that Reynolds number effects persist indefinitely for both mean velocity and higher-order statistics. True self-similarity seems to not be achieved at any high but finite Reynolds number in the flow types considered here (turbulent channel and pipe flows). All that has caused significant doubts on the classical picture of wall-bounded turbulence, although the precise functional shape of the mean-velocity profile and its correct Reynolds number dependence are still unknown for even the geometrically simplest albeit technically important turbulent flow, the canonical pipe and channel flow.

Because turbulence is not a closed problem, a large number of theories have been created to solve the topics addressed above. Beginning with the Izakson–Millikan [3,4] derivation of the standard logarithmic law, several asymptotic approaches were developed. One of the first higher-order theories extending the standard log law was advanced by Tennekes [5] who derived a second-order law for pipe flows. An early theory based on asymptotic methods was given by Yajnik [6]. This work basically led to asymptotic laws corresponding to the law of the wall, the logarithmic law, the velocity defect law, and the law of the wake. Mellor [7] extended Yajnik's work by considering an inviscid region as part of wall flow. The work by Mellor is reflected in detail in the textbooks by Gersten and Herwig [8] and Schlichting and Gersten [9]. In 1976, Afzal [10] published one of the first general higher-oder theories for the overlap layer of pipe and channel flows (see also Afzal and Yajnik [11]). Afzal's work is also the basis for the higher-order approach by Buschmann and Gad-el-Hak [12], considered here among others. A recent review of asymptotic expansions is given by Panton [13].

A key feature of wall turbulence is the complex, three-dimensional and instantaneous turbulent motion. This statement follows directly from experimental evidence presented in several recent papers (Adrian [14], Hutchins and Marusic [15], and Monty et al. [16]). The turbulent motion is subjected to viscous and inertial forces acting throughout the entire flow but with different intensities at different wall-normal positions. This assertion follows directly from the governing equations because there is no y position in the flow, except the wall itself, where one or the other term can be set identically zero. Nevertheless, as a zeroth-order approximation it is not unreasonable to split wall-bounded turbulent flow into two distinct albeit overlapping zones. This is the classical view that assumes an overlap region where both viscous and inertial forces can be neglected. Under this assumption the simple logarithmic law holds

$$u^+ = \frac{1}{\kappa}\ell_n(y^+) + B; \qquad u^+ = \frac{u}{u_\tau}; \qquad y^+ = \frac{yu_\tau}{\nu} \tag{1}$$

where κ denotes the Kármán constant, B is the additive constant, y is the wall-normal coordinate, and u is the mean velocity in the streamwise direction. Both κ and B are presumed to be independent of the Reynolds number. The superscript $+$ stands for normalization with wall variables, the friction velocity $u_\tau = \sqrt{\tau_w/\rho}$ and the fluid kinematic viscosity ν, where τ_w is the wall shear stress and ρ is the fluid density. The simple logarithmic law implies that the size of the eddies in the overlap region grows proportional to the distance from the wall (Adrian [14]), and that scaling based on wall variables alone is sufficient. The fact that several spanwise length scales are indeed growing linearly with distance from the wall was shown experimentally by Tomkins and Adrian [17]. However, an analysis of the stresses of turbulent channel and pipe flow conducted by

Received 6 February 2008; revision received 7 July 2008; accepted for publication 21 July 2008.

*Senior Researcher; Matthias.Buschmann@ilkdresden.de.
†Caudill Professor and Chair, Department of Mechanical Engineering. Associate Fellow AIAA.

Buschmann et al. [18] makes it clear that wall turbulence is also affected by outer scales.

The fact that inner-region turbulence is influenced by outer scales is well known and was discussed by several authors. DeGraaff and Eaton [19] introduced the so-called mixed scaling for zero-pressure-gradient turbulent boundary layers to cover the Reynolds number dependence of $\bar{u}'^2$. George and Castillo [20] found from asymptotic analysis that $\bar{u}'^2$ should be scaled employing u_e^2, where u_e denotes the velocity at the outer edge of the boundary layer. Recently, Morrison [21] examined the interaction of inner and outer regions and found that a "weak" asymptotic condition is needed to represent the increasing effect of outer-scale influence as the Reynolds number increases. He also stated very clearly that the inner–outer interaction is an intrinsically nonlinear process.

In this paper, we use several DNS databases and the results of two independent experiments to compare three leading theories that predict specific forms of the Reynolds-number-dependent mean-velocity profile. Direct numerical simulations are used more extensively herein because they provide the accuracy needed to validate the different theories. In contrast to previous work that focused on the mean-velocity data, herein we employ data of peak position and peak values of Reynolds shear stress, which provide a much more sensitive test to validate the different theories.

The three theories considered herein are the generalized logarithmic law advanced by Buschmann and Gad-el-Hak [12], the alternative logarithmic law by Wosnik et al. [22], and the power law by Barenblatt [23]. These theories are representative of the ongoing debate on wall-bounded turbulence. Other more recent theories such as the self-similar profile based on probability density functions by Tsuji et al. [24], the scaling laws based on Lie group or symmetry approaches by Khujadze and Oberlack [25], or the instantaneous log law based on an asymptotic analysis of the Navier–Stokes equation by Lundgren [26] are not considered here for two reasons: 1) these theories are aimed primarily at boundary-layer flows and not internal flows, and 2) the theories contain parameters, especially within the higher-order terms, which were not supplied by the original authors.

In the limit of infinite Reynolds number, both the generalized logarithmic law and Wosnik's logarithmic law lead to a logarithmic overlap region. For finite Reynolds numbers, neither law exhibits a "true overlap region" in which the inner or outer flow, or the overlap region itself, are Reynolds number independent. However, the Kármán number dependencies (representing the Reynolds number dependencies) and therefore the asymptotic behavior of both approaches is different. Barenblatt's ansatz is a Reynolds-number-dependent power law that never leads to a logarithmic state of the profile. All three approaches have in common that they show an explicit Reynolds number dependency. Note that the Kármán number is closely related to the mean-flow Reynolds number. None of these laws assumes true self-similarity in the same sense as the classical logarithmic law does. All of them are intended for finite Reynolds number flows and explicitly consider Reynolds number dependency.

The advantage of the generalized logarithmic law and Wosnik's logarithmic law compared with the combination of power law and classical logarithmic law proposed by McKeon et al. [27] is simply that the first two are "monolithic." They are based on one set of physical assumptions and follow from one mathematical derivation. From a practical point of view, these laws avoid the discontinuity that inevitably occurs at the matching point when two functions are stuck together. This is also true for the combination of inner and outer power laws proposed by Barenblatt et al. [28].

II. Evidence of Reynolds Number Dependency

Strictly speaking, the universal logarithmic law is valid only in the limit of infinite Reynolds number. For any other value, the Reynolds number dependency of the governing equations prevents strict self-similarity (meaning Reynolds-number-independent solutions). Experimental support for that theoretical argument comes from, for example, the superpipe data by McKeon et al. [27], which indicates that a universal logarithmic law does not emerge below a Reynolds number of 2.3×10^5. Our own view is that above this value, the Reynolds number dependency of the equations does not disappear, it is merely extremely weak and therefore not easy to detect experimentally. That weak effect is overwhelmed by experimental uncertainties, which, because of probe resolution issues, magnify at higher Reynolds numbers.

In a recent paper, Lundgren [26] conducted an expansion of the complete unsteady Navier–Stokes equations. Bypassing altogether Prandtl's boundary-layer simplifications, Lundgren's approach does not rely on any assumption with respect to the Reynolds shear stress. Resulting from his study is a composite expansion that extends beyond the classical Reynolds-number-independent overlap region

$$\langle u^+ \rangle = \frac{1}{\kappa} \ell_n(y^+) + \langle B_i \rangle + \frac{\langle B_{i,1} \rangle}{y^+} + \langle B_{o,1} \rangle Y + \cdots \tag{2}$$

where $B_{i,1}$ and $B_{o,1}$ are functions of normalized streamwise and wall-normal coordinates and of normalized time, angle brackets denote time averages, and $Y = y^+/\delta^+$. This most fundamental approach clearly reveals that the streamwise velocity profile depends on the Reynolds number in both wall and outer variables and that higher-order terms with respect to the wall-normal coordinate must be considered. The generalized logarithmic law proposed by Buschmann and Gad-el-Hak [12] has a similar structure but with a more generalized Reynolds number dependency. Of course, any logarithmic law can be approximated locally by a power law. But as Lundgren [26] pointed out, that only shows that power laws are rational approximations to the logarithmic law over a limited y^+ range.

Aside from the experimental evidence of Reynolds number dependency of the mean-velocity profile in the overlap layer, we present three arguments in support of the idea that both outer and inner scales are important throughout the entire wall-bounded flow:

1) From flow visualizations it is known that vortices connected with the wall reach far into the outer region (e.g., Head and Bandyopadhyay [29], Adrian et al. [30]), and that fluid structures from the outer region dive deep into the inner layer (e.g., Hites [31]). The most recent experiments in turbulent boundary layers by Hutchins and Marusic [15] confirmed the existence of long meandering "superstructures" extending more than 20δ in length in the logarithmic and the lower wake region, where δ is the boundary-layer thickness. Those structures leave their footprints deep into the near-wall region. Qualitatively similar structures up to 25 pipe radii or channel half-widths are reported by Monty et al. [16] for confined flows.

2) Any vortex occurring in the outer flow of a boundary layer or the core region of pipe and channel flow induces a velocity field that pervades the complete wall-bounded flowfield (Davidson [32]). The size of these eddies correlates with the boundary-layer thickness or channel half-width. Experimental support for that notion comes from Guala et al. [33] who found that large-scale motions having wavelengths of 2δ–3δ occur throughout the entire layer.

3) Analyzing the mean-momentum equation for pipe and channel flows

$$0 = \frac{\mathrm{d}p^+}{\mathrm{d}x^+} - \frac{\mathrm{d}(\overline{u'v'})^+}{\mathrm{d}y^+} + \frac{\mathrm{d}^2u^+}{\mathrm{d}y^{+2}} \tag{3}$$

it becomes clear that at the peak position of the Reynolds shear stress, the second term on the right-hand side vanishes. The Reynolds-shear-stress gradient and not the Reynolds shear stress itself is what appears in the momentum equation, and therefore the Reynolds-stress term is entirely absent at its peak position y_p. In the vicinity of this point, which, at high Reynolds numbers is located well within the classical logarithmic region, the pressure gradient term must be balanced mostly by the viscous term. According to Sreenivasan and Sahay [34], this observation provides a mechanism by which viscous effects play an important role in regions traditionally thought to be inviscid (i.e., inertial). This throws grave doubt on the validity of the classical matching principle and all of its consequences. Sreenivasan [35] termed the region in the immediate vicinity of y_p the "critical

layer." Several years before that, Long and Chen [36] identified this region as a "mesolayer."

Taken together, the above arguments strongly support the idea of scaling near-wall turbulence, including the mean-velocity profile, with both inner and outer variables. Therefore, the ratio of inner to outer length scales—the Kármán number $\delta^+ = u_\tau \delta/\nu$, where δ is the boundary-layer thickness, the pipe radius, or the channel half-width —should play an important role. One of the fundamental questions is whether there are regions where the turbulence exhibits universal features such as a constant Reynolds-stress layer, $-\overline{u'v'} \approx u_\tau^2$. The three theories considered herein (generalized logarithmic law, alternative logarithmic law, and Barenblatt's power law) answer that question in the negative sense and indicate a Kármán number dependency. However, in all three cases this dependency, and hence the asymptotic structure of the approach, is different.

III. Basic Idea of the Analysis

The scope of our analysis is to validate or falsify the Kármán number dependencies of the three approaches considered. All of them rely on statistics and therefore have to be validated accordingly. For that purpose, we analyze the asymptotic structure of all three approaches with respect to peak position and peak value of the Reynolds shear stress. Both parameters are very distinct features of the statistics of wall-bounded flows. In the theories considered, both follow implicitly from the physical assumptions employed to close the turbulence problem. This is not directly apparent because those quasi-closure models are hidden in the approaches either as a certain form of gauge functions (Buschmann and Gad-el-Hak [12]), in the basic assumptions constituting the asymptotic invariance principle (Wosnik et al. [22]), or by a priori assuming a power law (Barenblatt [23]).

All three theories have in common the implicit assumption that the classical logarithmic law is not valid if the Reynolds number is finite, which implies that the peak value of the shear stress is not exactly unity. The more that peak deviates from 1, the less accurate the classical logarithmic law is, and hence the need for higher-order corrections. Certain researchers claim that if the peak value is below a certain value, then the logarithmic law is not valid below a certain Reynolds number (see, for example, Zanoun et al. [37]). The difference between this claim and the theories considered herein is that the former demands a sharp transition. Either logarithmic law is valid or not valid. On the other hand, the latter considers that transition as a continuum from the minimum Reynolds number for turbulence, $Re_{\min}$, to infinite Reynolds number. At $Re_{\min}$, the logarithmic law is a poor approximation, and at infinite Reynolds number it is the common part of the inner and outer regions. However, for any finite Reynolds number the classical logarithmic law is not sufficient to describe the flow properly. For example, at $Re_{\min}$ one needs an infinite number of terms in the generalized logarithmic law, whereas at infinite Reynolds number one needs only the zeroth order and the classical logarithmic law is restored.

First of all, we have to answer the question whether or not these theories are in principle valid around the shear-stress peak. Two points have to be kept in mind when answering this question. First, the peak position is a function of the Kármán number as amply demonstrated by Sreenivasan and Sahay [34]:

$$y_p^+ = (1.8 \pm 0.2)\delta^{+0.5} \tag{4}$$

and, second, all three theories are so far only validated employing mean-velocity profiles. From these investigations, however, at least several clues for answering the above question can be drawn. Note that Eq. (4) can be derived from the mean-momentum equation for internal flows assuming the standard log law and the local-equilibrium hypothesis.

Investigating the superpipe data by McKeon et al. [27], Buschmann and Gad-el-Hak [1] found that their mean-velocity profiles are well represented by the generalized logarithmic law down to $y^+ \approx 80$ (see Fig. 22 of the latter paper). Morrison et al. [38] give, for pipe flow, a peak position of the Reynolds shear stress varying with the Kármán number according to

$$y_p^+ = (1.5 \pm 0.2)\delta^{+0.5} \tag{5}$$

Combining both results suggests that the generalized logarithmic law (GLL) covers the mean-velocity profile of pipe flow at least for $\delta^+ > 3000$.

An analysis for turbulent boundary layers with zero pressure gradient (Buschmann and Gad-el-Hak [12]) showed a near-perfect agreement between the experimental data and the generalized logarithmic law above $y^+ \approx 25$. A comparable lower border of $y^+ \approx 30$ was reported by Wosnik et al. [22] for their alternative logarithmic law employing DNS channel flow data and the first superpipe data set by Zagarola [39]. In a previous study, Sreenivasan and Sahay [34] used Barenblatt's power law without any restrictions with respect to the y^+ coordinate. That a power law region below the logarithmic region may indeed exist was shown by McKeon et al. [27]. The y^+ region reported for pipe flow on page 145 of that reference is between $50 < y^+ < 300$. To summarize, all of these investigations indicate that the three theories under consideration may well be applicable in the vicinity of the Reynolds-shear-stress peak.

Finally, it has to be emphasized that the entire analysis herein focuses on pipe and channel flows. The results will not be suitable therefore for zero-pressure-gradient turbulent boundary layers and other types of semiconfined flows. The reason is simply the different types of Kármán number dependencies that have to be considered for the different flows.

IV. Data Selection and Processing

The analysis undertaken herein requires a careful selection of data. Our main hypothesis is that any Reynolds number effect will be extremely weak at high Reynolds numbers. Additionally, we argue that nearly all available experimental data having low Kármán number show a scatter that excludes them from an unequivocal detection of higher-order effects. Therefore, we focus mainly on DNS of channel flow (see Table 1). Special care was taken when selecting DNS data for very low Kármán numbers to exclude any

Table 1 Compiled data covering the Kármán number range between 64 and 5.3×10^5. CH: channel flow; PF: pipe flow; DNS: direct numerical simulations; EXP: experiment

Authors	Kármán numbers	Type	Symbol
Abe et al. [45]	180, 365, 640, 1020	CH DNS	Black star
Duggleby et al. [46]	150	PF DNS	Gray square
Hoyas & Jimenez [47]	180, 550, 934, 2006	CH DNS	Gray star
Hu et al. [48]	90, 130, 180, 360, 720, 1440	CH DNS	Black triangle
Iwamoto et al. [49]	110, 150, 298, 395, 642 120, 160, 180, 235, 589, 1000	CH DNS	Black square
Laadhari [50]	1006, 1461	CH DNS	Gray triangle
Moser et al. [51]	178, 392, 587	CH DNS	Gray diamond
Tsukahara et al. [52]	64, 70, 80, 110, 150	CH DNS	Black diamond
McKeon et al. [27]	$(1.8 \times 10^3 \le \delta^+ \le 5.3 \times 10^5)$	PF EXP	Black circle
Zanoun [40]	$(1.2 \times 10^3 \le \delta^+ \le 4.8 \times 10^3)$	CH EXP	Gray circle

results that might be affected by an insufficiently small calculation domain. This ensures that all relevant scales for the turbulence shear stress are captured. For the high-Reynolds-number range, we employ the superpipe data by McKeon et al. [27] and the channel flow data by Zanoun [40]. To obtain position and value of the Reynolds shear-stress peak both experimental data sets were differentiated. Special attention is given to the determination of this gradient because the data have been taken nonequidistantly in y^+. Therefore a weighted gradient formulation (Grossmann and Roos [41]) should represent the true gradient very accurately

$$\frac{\partial u^+}{\partial y^+} = f_a \frac{u_i^+ - u_{i-1}^+}{y_i^+ - y_{i-1}^+} + f_b \frac{u_{i+1}^+ - u_i^+}{y_{i+1}^+ - y_i^+};$$
$$f_a = \frac{y_{i+1}^+ - y_i^+}{y_{i+1}^+ - y_{i-1}^+}; \qquad f_b = \frac{y_i^+ - y_{i-1}^+}{y_{i+1}^+ - y_{i-1}^+} \tag{6}$$

V. Mathematical Considerations

The integrated mean-momentum equation for a fully developed, turbulent pipe or channel flow reads

$$\tau^+ = 1 - \frac{y^+}{\delta^+} - \frac{\mathrm{d}u^+}{\mathrm{d}y^+} \tag{7}$$

The Reynolds-shear-stress τ^+ remains unknown until a mean-velocity profile is assumed. The three mean-velocity profiles we consider herein are 1) the generalized logarithmic law (GLL, subscript G) derived by Buschmann and Gad-el-Hak [12]:

$$u_G^+ = \left[\sum_{i=0}^{\infty} \frac{1}{\kappa_i} \frac{1}{\delta^{+i}}\right] \ell_n(y^+ + a^+) + \sum_{i=0}^{\infty} \frac{1}{\delta^{+i}} C_i + \sum_{i=1}^{m} \frac{1}{\delta^{+i}} \sum_{j=1}^{i} B_{i,j} y^{+j} \tag{8}$$

2) the alternative logarithmic law (WLL, subscript W) derived by Wosnik et al. [22]:

$$u_W^+ = \left[\frac{1}{\kappa_\infty} - \sum_{i=1}^{n} \frac{(1 - i + \alpha) A_i}{\ell_n (D\delta^+)^{(i+\alpha)}}\right] \ell_n[y^+ + a^+(\delta^+)] + B_i(\delta^+) \tag{9}$$

and 3) the power law (BPL, subscript B) proposed by Barenblatt [23]:

$$u_B^+ = \gamma(\delta^+) y^{+\beta(\delta^+)} \tag{10}$$

Introducing the different velocity profiles into Eq. (7) delivers the associated Reynolds-shear-stress distributions $\tau^+(y^+, \delta^+)$ in the vicinity of its peak. Differentiating those leads then to the equations for the peak position, which is shown here for GLL and WLL up to second order. Sreenivasan and Sahay [34] give an equivalent relation up to arbitrary order Eq. (13) for Barenblatt's power law:

$$y_{pG}^+ = \frac{\delta^{+1/2}}{\kappa_0^{1/2}} \left[1 + \underline{\frac{1}{\delta^+} \frac{\kappa_0}{\kappa_1}}\right]^{1/2} - a^+ \tag{11}$$

$$y_{pW}^+ = \frac{\delta^{+1/2}}{\kappa_\infty^{1/2}} \left[1 - \underline{\kappa_\infty \frac{\alpha A_1}{\ell_n (D\delta^+)^{(1+\alpha)}}}\right]^{1/2} - a^+(\delta^+) \tag{12}$$

$$y_{pB}^+ = \lambda \delta^{+1/2} \left[1 + \underline{\lambda_{11} \frac{\ell_n\{\ell_n(\delta^+)\}}{\ell_n(\delta^+)}}\right] \tag{13}$$

The leading-order term of all approaches is of the form $a\delta^{+1/2}$, which resembles the equivalent result derived from the classical logarithmic law (1). An additional first-order correction follows from the additive term a^+ inside the logarithmic terms of GLL and WLL. The second-order terms, underlined in Eqs. (11–13), are different in each case and ultimately are a consequence of the underlying physical assumptions.

Physical and numerical experiments clearly show that for any finite Kármán number, the maximum Reynolds shear stress is smaller than unity (Gad-el-Hak and Bandyopadhyay [42]). Therefore, a shear-stress correction term is written as

$$\Delta(\delta^+) = 1 - \tau_{\max}^+(\delta^+) \tag{14}$$

Introducing the second-order representation of the shear-stress position of Eqs. (11–13) into Eq. (14) delivers the shear-stress correction for GLL and WLL. An analogous relation for Barenblatt's power law (17) was derived by Sreenivansan and Sahay [34]:

$$\Delta_G(\delta^+) = \frac{1}{\kappa_0^{1/2}} \frac{1}{\delta^{+1/2}} [K_G^{\frac{1}{2}} + K_G^{-\frac{1}{2}}] + \frac{1}{\delta^+} [B_{11} - a^+]$$
$$+ \frac{1}{\delta^{+3/2}} \left[2 \frac{B_{22}}{\kappa_0^{1/2}} K_G^{\frac{1}{2}} + \frac{\kappa_0^{\frac{1}{2}}}{\kappa_1} K_G^{-\frac{1}{2}}\right] + O\left[\frac{1}{\delta^{+2}}\right] \tag{15}$$

where

$$K_G = 1 + \frac{1}{\delta^+} \frac{\kappa_0}{\kappa_1}$$

$$\Delta_W(\delta^+) = \frac{1}{\kappa_\infty^{1/2}} \frac{1}{\delta^{+1/2}} [K_W^{\frac{1}{2}} + K_W^{-\frac{1}{2}}] - \frac{\kappa_\infty^{1/2}}{\delta^{+1/2}} \frac{1}{K_W^{1/2}} \frac{\alpha A_1}{\ell_n (D\delta^+)^{(1+\alpha)}}$$
$$- \frac{\kappa_\infty^{1/2}}{\delta^{+1/2}} \frac{1}{K_W^{1/2}} \frac{(1+\alpha) A_2}{\ell_n (D\delta^+)^{(2+\alpha)}} + O\left[\frac{1}{\ell_n (\delta^+)^{3+\alpha}}\right] \tag{16}$$

where

$$K_W = 1 - \kappa_\infty \frac{\alpha A_1}{\ell_n (D\delta^+)^{(1+\alpha)}}$$

and

$$\Delta_B(\delta^+) = \frac{a_0}{\delta^{+1/2}} + \frac{a_{11}}{\delta^{+1/2}} \frac{\ell_n[\ell_n(\delta^+)]}{\ell_n(\delta^+)} + \frac{a_{21}}{\delta^{+1/2}} \frac{1}{\ell_n(\delta^+)} + O[\text{h.o.t.}] \tag{17}$$

For $\delta^+ \to \infty$, the leading-order terms of all three attempts have the form $\beta/\delta^{+1/2}$, which mirrors the logarithmic first-order behavior of the mean-velocity profile in the vicinity of y_p^+. The task is now to identify which of the proposed Kármán number dependencies correctly represents the higher-order correction of the peak value of the Reynolds shear stress.

VI. Results

In a first step it is assumed that second- and higher-order effects are negligible for very high Kármán numbers. Equations (15–17) reduce then to

$$\Delta(\delta^+) = \frac{\beta}{\delta^{+1/2}}; \qquad \beta_G = \frac{2}{\kappa_0^{1/2}}; \qquad \beta_W = \frac{2}{\kappa_\infty^{1/2}}; \qquad \beta_B = a_0 \tag{18}$$

The superpipe data from McKeon et al. [27] are now used to predict the coefficient β.

The inset of Fig. 1 depicts a perfect straight-line fit of the superpipe data. The computed β value of 3.043 is very close to 3.1 ± 0.1, the value proposed by Sreenivasan and Sahay [34]. Calculating κ from this β value leads to 0.432, which is only 2.6% higher than the value derived by McKeon et al. [27] from separate measurements of pressure drop and velocity collapse using inner and outer variables. Our value is also in excellent agreement with $\kappa_\infty = 0.43$, proposed by George [43] for pipe flows. Figure 1 illustrates that the concordance between data and first-order correction is good above $\delta^+ \approx 800$, which is also confirmed by the channel flow data by Zanoun [40]. The departure from the leading-order solution due to higher-order effects increases markedly below this threshold.

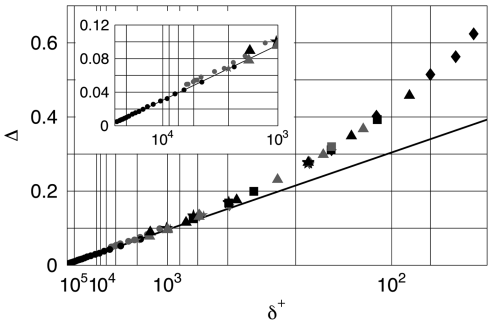

Fig. 1 First-order correction of Reynolds shear-stress peak value (see Table 1 for symbols). The abscissa is transformed according to the forecasted Kármán number dependency, $1/\delta^{+1/2}$. The solid line indicates a first-order fit following from superpipe data (solid circles in the inset box).

In the second step the difference $\Delta^*(\delta^+)$ between the leading-order correction and the actual value of $\Delta(\delta^+)$ is predicted. This departure should be described to leading order by the second-order terms provided in Eqs. (15–17). To clearly delineate the dependency, this departure is plotted versus abscissas that are transformed according to the forecasted Kármán number dependency. For GLL this is $1/\delta^+$; for WLL it is $1/\delta^{+1/2}/K_W^{1/2}/\ell_n(D\delta^+)^{(1+\alpha)}$; and for BPL it is $\ell_n[\ell_n(\delta^+)]/\delta^{+1/2}/\ell_n(\delta^+)$. In case the second-order correction is sufficient to cover the remaining Kármán number effects properly, all data points should order along a straight line. Note that no curve fit is needed to verify the δ^+ range where the second-order correction is sufficient. Figure 2 demonstrates that the second-order correction works fine down to about $\delta^+ \approx 350$ for WLL and down to $\delta^+ \approx 400$ for GLL and BPL. A least-square fit for GLL in the appropriate region gives a slope of 5.14. The slope for WLL follows from the parameters $\alpha = -0.932$, $D = 1$, and $A_1 = 0.145$ given by George [43]. For Barenblatt's power law, a slope of 0.71 is found, which is slightly lower than the value of 0.93 proposed by Sreenivasan and Sahay [34]. For lower values of δ^+, all attempts show again a significant departure from the straight line indicating a need to consider third- and higher-order Kármán number corrections.

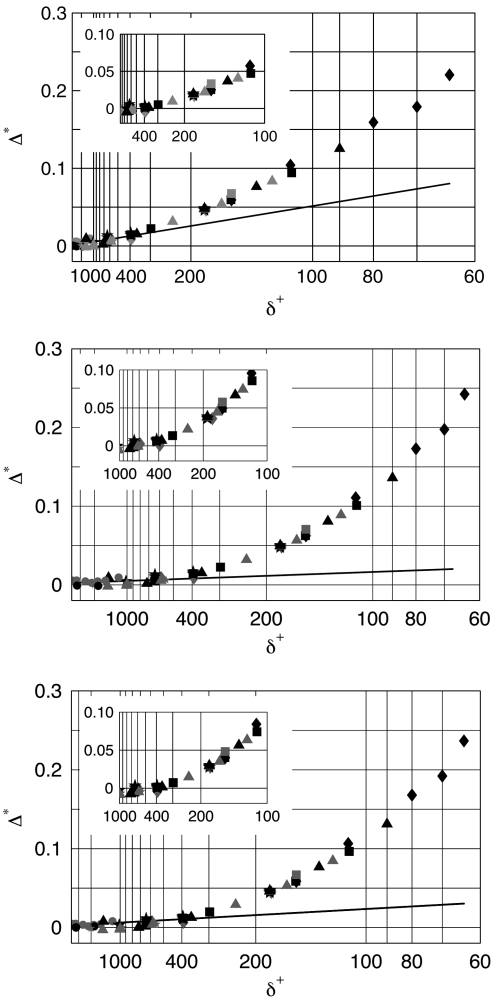

Fig. 2 Second-order correction of peak value of Reynolds shear stress for GLL (top figure), WLL (center figure), and BPL (bottom figure). Symbols are described in Table 1. Abscissae are transformed according to the forecasted Kármán number dependency for each theory. Solid lines show linear fits. Insets show a departure from the linear fit for a medium Kármán number.

In the final step the procedure from the second step is repeated. This time the remaining departure $\Delta^{**}(\delta^+)$ between the second-order correction and the actual $\Delta(\delta^+)$ values is predicted. Once again, this difference is plotted versus abscissas that are transformed according to the functional Kármán number dependency of the third-order terms in Eqs. (15–17). Assuming that the factors appearing in K_G are of the same order of magnitude, the abscissa for GLL follows $1/\delta^{+3/2}(K_G^{1/2} + K_G^{-1/2})$. For WLL, the abscissa is scaled as $1/\delta^{+1/2}/K_W^{1/2}\,\ell_n(D\delta^+)^{(2+\alpha)}$, and for BPL, it is $1/\delta^{+1/2}/\ell_n(\delta^+)$.

Again it is expected that in regions where the third-order correction is sufficient, all data points would be ordered along a straight line. As shown in the upper plot of Fig. 3, this is obviously the case for the generalized logarithmic law over the entire Kármán

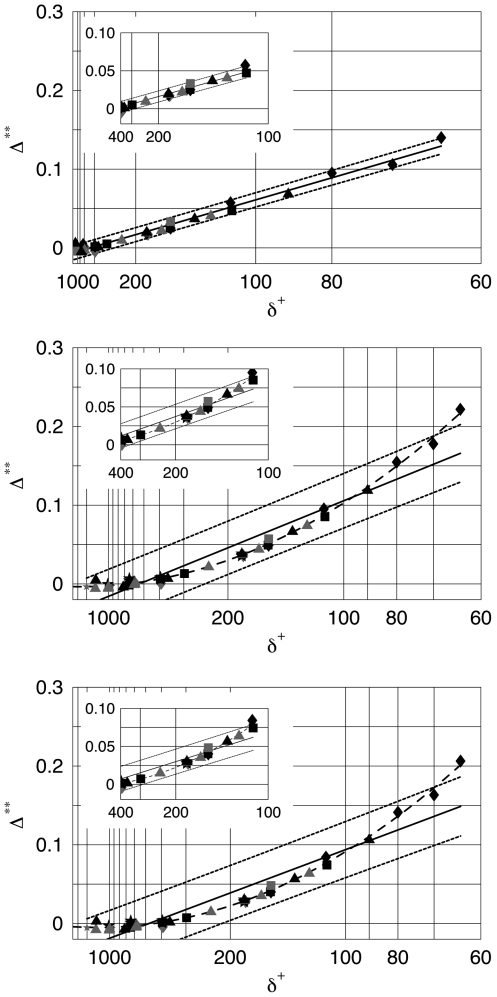

Fig. 3 Third-order correction of peak value of Reynolds shear stress for GLL (top figure), WLL (center figure), and BPL (bottom figure). Symbols are described in Table 1. Abscissae are transformed according to the forecasted Kármán number dependency for each theory. Solid lines show linear fits and dotted lines show the 95% confidence interval. Broken lines in the two lower plots indicate a parabolic fit. The insets show the same as the large plots but with a fitting region limited to Kármán numbers higher than 100.

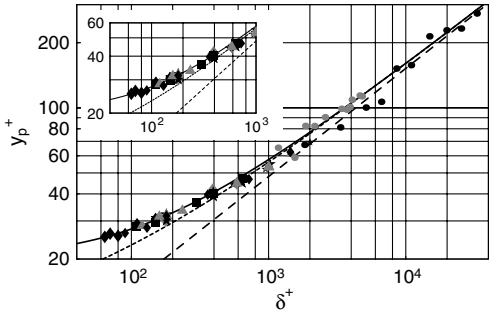

Fig. 4 Peak position of Reynolds shear stress according to the generalized logarithmic law. Broken line: first order without first-order correction term a^+; dotted line: complete first-order correction; solid line: second-order correction.

number range investigated. The third-order corrections of Wosnik's alternative logarithmic law and Barenblatt's power law (respectively, middle and lower plots of Fig. 3) are ordered almost on a parabola. The linear fit fails in the sense that in both cases above $\delta^+ \approx 100$, the data points lie below the straight line. The 95%-confidence interval is in both cases significantly larger than that for GLL.

Note that the lowest Kármán number considered here is 64 (Reynolds number based on bulk velocity $Re_b = 1844$), which is very close to relaminarization. A reliable conclusion for fully developed turbulent channel and pipe flows might therefore only be drawn down to $\delta^+ \approx 100$ ($Re_b \approx 2960$). Therefore, the analysis is repeated excluding data having δ^+ smaller than 100, and the results depicted in the insets in Fig. 3. Again an excellent collapse of all data points along a straight line is obtained for GLL. This clearly indicates that the data follow the Kármán number dependency forecasted by the generalized logarithmic law. Furthermore, the figure for GLL shows that Kármán number effects higher than third order are marginal and are even overshadowed by the minuscule numerical errors of the DNS data. As for the analysis of the entire Kármán number range, the linear fit fails for WLL and BPL, which indicates that the Kármán number effects identified are not in agreement with their respective theories.

By adapting the κ_1 value of $1/150$ found by Jiménez and Moser [44], Eq. (11) is now specified as

$$y_{pG}^+ = 1.521\delta^{+1/2}K_G^{1/2} + 8 \tag{19}$$

with $K_G = 1 + (64.8/\delta^+)$. The shear-stress correction (15) follows

$$\Delta_G(\delta^+) = 1.52\frac{1}{\delta^{+1/2}}[K_G^{\frac{1}{2}} + K_G^{-\frac{1}{2}}] + 5.14\frac{1}{\delta^+} + 32.75\frac{1}{\delta^{+3/2}}[K_G^{\frac{1}{2}} + K_G^{-\frac{1}{2}}] + O\left[\frac{1}{\delta^{+2}}\right] \tag{20}$$

Figure 4 shows the peak position of the Reynolds shear stress according to the generalized logarithmic law. It can be seen clearly that higher-order effects become significant below the Kármán number of about 1000. The first-order y^+ correction represented by a^+ covers these effects only partially. Not until the second-order δ^+ correction is introduced is a proper fit of the y_p^+ data achieved.

VII. Conclusions

Three different theories that predict the mean-velocity profile in the overlap region of wall-bounded turbulent flows are compared. All theories demand the inclusion of higher-order effects with respect to the ratio of outer to inner length scales. However, the functional representation of this dependency is different in each case. We employ data of peak position and values of Reynolds shear stress provided by channel flow DNS and pipe and channel flow experiments to validate these dependencies. In contrast to previous work that focused on the mean velocity, the data of peak position and values of Reynolds shear stress employed herein provide a much more sensitive test to validate the different theories.

It is found that both the peak position and peak value of the Reynolds shear stress follow the reciprocal of powers of the Kármán number, rather than the reciprocal of powers of the logarithm of the same. Two conclusions are drawn from that finding. The first one is rather a qualitative statement that even regions very close to the wall are affected by flow phenomena that scale directly with outer variables and not with the much smaller logarithm of these scales. The second conclusion tells something about the quality of the disappearance of the δ^+ dependency. Because of the fact that peak position and value follow $1/\delta^+$ rather than $1/\ell_n(\delta^+)$, any Kármán number effects will die out very rapidly. A primary finding of this study is that these effects are clearly visible in the near-wall Reynolds shear stress. Therefore, they must also be considered in the near-wall mean-velocity profile.

Note added in proof: A recent publication by Wu and Moin [53] came to our attention as this paper was going to press. Two of the highlights of their article are the finding that direct numerical simulation pipe-flow realizations having the highest Reynolds number ever achieved with DNS ($Re_D = 44,000$; $\delta^+ = 1142$) do not support the theory advanced by Wosnik et al. [22], and that the mean-velocity profiles "exhibit limited rather than extended power-type behavior." Both findings strongly support our results. We could readily show that the reason for the first finding by Wu and Moin [53] is not the inner additive constant of advanced logarithmic laws, but rather the particular functional form of the Kármán-number dependency proposed by Wosnik et al. [22].

References

[1] Buschmann, M. H., and Gad-el-Hak, M., "Recent Developments in Scaling of Wall-Bounded Flows," *Progress in Aerospace Sciences*, Vol. 43, 2007, pp. 419–467.

[2] Gad-el-Hak, M., "The Last Conundrum. Guest Editorial," *Applied Mechanics Reviews*, Vol. 50, No. 12, 1997, Pt. 1, pp. i–ii.

[3] Izakson, A. A., "Formula for the Velocity Distribution Near a Wall," *Zhurnal Eksperimental'noi i Teoreticheskoi Fiziki*, Vol. 7, 1937, pp. 919–924.

[4] Millikan, C. B., "A Critical Discussion of Turbulent Flows in Channels and Circular Tubes," *Proceedings of the Fifth International Congress on Applied Mechanics*, edited by J. P. Den Hartog and H. Peters, Wiley, New York, 1938, pp. 386–392.

[5] Tennekes, H., "Outline of a Second-Order Theory of Turbulent Pipe Flow," *AIAA Journal*, Vol. 6, No. 9, Sept. 1968, pp. 1735–1740. doi:10.2514/3.4852

[6] Yajnik, K. S., "Asymptotic Theory of Turbulent Shear Flows," *Journal of Fluid Mechanics*, Vol. 42, No. 2, 1970, pp. 411–427. doi:10.1017/S0022112070001350

[7] Mellor, G. L., "The Large Reynolds Number, Asymptotic Theory of Turbulent Boundary Layers," *International Journal of Engineering Science*, Vol. 10, No. 10, 1972, pp. 851–873. doi:10.1016/0020-7225(72)90055-9

[8] Gersten, K., and Herwig, H., *Strömungsmechanik, Fundamentals and Advances in the Engineering Science*, Verlag Vieweg, Wiesbaden, Germany, 1992.

[9] Schlichting, H., and Gersten, K., *Grenzschicht-Theorie*, 9th ed, Springer, Berlin, 1997.

[10] Afzal, N., "Millikan's Argument at Moderately Large Reynolds Number," *Physics of Fluids*, Vol. 19, No. 4, 1976, pp. 600–602. doi:10.1063/1.861498

[11] Afzal, N., and Yajnik, K., "Analysis of Turbulent Pipe and Channel Flows at Moderately Large Reynolds Number," *Journal of Fluid Mechanics*, Vol. 61, No. 1, 1973, pp. 23–31. doi:10.1017/S0022112073000546

[12] Buschmann, M. H., and Gad-el-Hak, M., "Generalized Logarithmic Law and its Consequences," *AIAA Journal*, Vol. 41, No. 1, Jan. 2003, pp. 40–48. doi:10.2514/2.1911

[13] Panton, R. L., "Review of Wall Turbulence as Described by Composite Expansions," *Applied Mechanics Reviews*, Vol. 58, Jan. 2005, pp. 1–36. doi:10.1115/1.1840903

[14] Adrian, R. J., "Hairpin Vortex Organization in Wall Turbulence," *Physics of Fluids*, Vol. 19, April 2007, p. 041301. doi:10.1063/1.2717527

[15] Hutchins, N., and Marusic, I., "Evidence of Very Long Meandering Features in the Logarithmic Region of Turbulent Boundary Layers,"

Journal of Fluid Mechanics, Vol. 579, May 2007, pp. 1–28. doi:10.1017/S0022112006003946

[16] Monty, J. P., Stewart, J. A., Williams, R. C., and Chong, M. S., "Large-Scale Features in Turbulent Pipe and Channel Flows," *Journal of Fluid Mechanics*, Vol. 589, Oct. 2007, pp. 147–156. doi:10.1017/S002211200700777X

[17] Tomkins, C. D., and Adrian, R. J., "Spanwise Structure and Scale Growth in Turbulent Boundary Layers," *Journal of Fluid Mechanics*, Vol. 490, Aug. 2003, pp. 37–74. doi:10.1017/S0022112003005251

[18] Buschmann, M. H., Indinger, Th., and Gad-el-Hak, M., "Near-Wall Behavior of Turbulent Wall-Bounded Flows," AIAA Paper 2008-4236, 2008.

[19] DeGraaff, D. B., and Eaton, J. K., "Reynolds-Number Scaling of the Flat-Plate Turbulent Boundary Layer," *Journal of Fluid Mechanics*, Vol. 422, Nov. 2000, pp. 319–346. doi:10.1017/S0022112000001713

[20] George, W. K., and Castillo, L., "Zero-Pressure-Gradient Turbulent Boundary Layer," *Applied Mechanics Reviews*, Vol. 50, No. 12, Pt. 1, 1997, pp. 689–729.

[21] Morrison, J. F., "The Interaction Between Inner and Outer Regions of Turbulent Wall-Bounded Flow," *Philosophical Transactions of the Royal Society of London, Series A: Mathematical and Physical Sciences*, Vol. 365, Jan. 2007, pp. 683–698. doi:10.1098/rsta.2006.1947

[22] Wosnik, M., Castillo, L., and George, W. K., "A Theory for Turbulent Pipe and Channel Flows," *Journal of Fluid Mechanics*, Vol. 421, Nov. 2000, pp. 115–145. doi:10.1017/S0022112000001385

[23] Barenblatt, G. I., "Scaling Laws for Fully Developed Turbulent Shear Flows. Part 1. Basic Hypotheses and Analysis," *Journal of Fluid Mechanics*, Vol. 248, April 1993, pp. 513–520. doi:10.1017/S0022112093000874

[24] Tsuji, Y., Lindgren, B., and Johansson, A. V., "Self-Similar Profile of Probability Density Functions in Zero-Pressure Gradient Turbulent Boundary Layers," *Fluid Dynamics Research*, Vol. 37, 2005, pp. 293–316. doi:10.1016/j.fluiddyn.2005.06.003

[25] Khujadze, G., and Oberlack, M., "New Scaling Laws in ZPG Turbulent Boundary Layer Flow," *Fifth International Symposium on Turbulence and Shear Flow Phenomena*, edited by R. Friedrich, N. A. Adams, J. K. Eaton, J. A. C. Humphrey, N. Kasagi, and M. A. Leschziner, Technical University of Münich, Münich, Germany, 2007 [CD-ROM].

[26] Lundgren, T. S., "Asymptotic Analysis of the Constant Pressure Turbulent Boundary Layer," *Physics of Fluids*, Vol. 19, May 2007, p. 055105. doi:10.1063/1.2723152

[27] McKeon, B. J., Li, J., Jiang, W., Morrison, J. F., and Smits, A. J., "Further Observations on the Mean Velocity Distribution in Fully Developed Pipe Flow," *Journal of Fluid Mechanics*, Vol. 501, Feb. 2004, pp. 135–147. doi:10.1017/S0022112003007304

[28] Barenblatt, G. I., Chorin, A. J., and Prostokishin, V. M., "Self-Similar Intermediate Structures in Turbulent Boundary Layers at Large Reynolds Number," *Journal of Fluid Mechanics*, Vol. 410, May 2000, pp. 263–283. doi:10.1017/S0022112099008034

[29] Head, M. R., and Bandyopadhyay, P. R., "New Aspects of Turbulent Boundary-Layer Structure," *Journal of Fluid Mechanics*, Vol. 107, April 1981, pp. 297–338. doi:10.1017/S0022112081001791

[30] Adrian, R. J., Meinhart, C. D., and Tomkins, C. D., "Vortex Organization in the Outer Region of the Turbulent Boundary Layer," *Journal of Fluid Mechanics*, Vol. 422, Nov. 2000, pp. 1–54. doi:10.1017/S0022112000001580

[31] Hites, M. H., "Scaling of High Reynolds Number Turbulent Boundary Layers in the National Diagnostic Facility," Ph.D. Thesis, Illinois Institute of Technology, Chicago, IL, 1997.

[32] Davidson, P. A., *Turbulence: An Introduction for Scientists and Engineers*, Oxford Univ. Press, London, England, United Kingdom, 2004.

[33] Guala, M., Hommema, S. E., and Adrian, R., "Large-Scale and Very-Large-Scale Motions in Turbulent Pipe Flow," *Journal of Fluid Mechanics*, Vol. 554, April 2006, pp. 521–542. doi:10.1017/S0022112006008871

[34] Sreenivasan, K. R., and Sahay, A., "The Persistence of Viscous Effects in the Overlap Region, and the Mean Velocity in Turbulent Pipe and Channel Flows," *Self-Sustaining Mechanisms of Wall Turbulence*, edited by R. Panton, Computational Mechanics Publications, Southampton, United Kingdom, 1997, pp. 253–272.

[35] Sreenivasan, K. R., "A Unified View of the Origin and Morphology of the Turbulent Boundary Layer Structure," *Turbulence Management and Relaminarisation*, edited by H. W. Liepmann, and R. Narasimha, Springer–Verlag, Berlin, 1987, pp. 37–61.

[36] Long, R. R., and Chen, T.-C., "Experimental Evidence for the Existence of the 'Mesolayer' in Turbulent Systems," *Journal of Fluid Mechanics*, Vol. 105, April 1981, pp. 19–59. doi:10.1017/S0022112081003108

[37] Zanoun, E.-S., Durst, F., and Nagib, H., "Evaluating the Law of the Wall in Two-Dimensional Fully Developed Turbulent Channel Flow," *Physics of Fluids*, Vol. 15, Oct. 2003, pp. 3079–3089. doi:10.1063/1.1608010

[38] Morrison, J. F., McKeon, B. J., Jiang, W., and Smits, A. J., "Scaling of the Streamwise Velocity Component in Turbulent Pipe Flow," *Journal of Fluid Mechanics*, Vol. 508, June 2004, pp. 99–131. doi:10.1017/S0022112004008985

[39] Zagarola, M. V., "Mean Flow Scaling in Turbulent Pipe Flow," Ph.D. Thesis, Princeton Univ., Princeton, NJ, 1996.

[40] Zanoun, E.-S., "Answers to Some Open Questions in Wall-Bounded Laminar and Turbulent Shear Flows," Ph.D. Thesis, Universität Erlangen-Nürnberg, Germany, 2003.

[41] Grossmann, C., and Roos, H.-G., *Numerik der Partiellen Differentialgleichungen*, B. G. Teubner, Stuttgart, Germany, 1994.

[42] Gad-el-Hak, M., and Bandyopadhyay, P. R., "Reynolds Number Effects in Wall-Bounded Flows," *Applied Mechanics Reviews*, Vol. 50, No. 8, 1994, pp. 307–365.

[43] George, W. K., "Is There a Universal Log Law for Turbulent Wall-Bounded Flows?," *Philosophical Transactions of the Royal Society of London, Series A: Mathematical and Physical Sciences*, Vol. 365, Jan. 2007, pp. 789–806. doi:10.1098/rsta.2006.1941

[44] Jiménez, J., and Moser, R. D., "What are we learning from simulating wall turbulence?," *Philosophical Transactions of the Royal Society of London, Series A: Mathematical and Physical Sciences*, Vol. 365, Jan. 2007, pp. 715–732. doi:10.1098/rsta.2006.1943

[45] Abe, H., Kawamura, H., and Matsuo, Y., "Surface Heat-Flux Fluctuations in a Turbulent Channel Flow up to $Re_\tau = 1020$ with $Pr = 0.025$ and 0.71," *International Journal of Heat and Fluid Flow*, Vol. 25, 2004, pp. 404–419. doi:10.1016/j.ijheatfluidflow.2004.02.010

[46] Duggleby, A., Ball, K. S., and Paul, M. R., "Dynamics of Propagating Turbulent Pipe Flow Structures. Part 1: Effect of Drag Reduction by Spanwise Wall Oscillation," 2007, arXiv:physics/0608258v3, pp. 1–11.

[47] Hoyas, S., and Jimenez, J., "Scaling of Velocity Fluctuations in Turbulent Channels up to $Re_\tau = 2003$," *Physics of Fluids*, Vol. 18, 2006, p. 011702. doi:10.1063/1.2162185

[48] Hu, Z. W., Morfey, C. L., and Sandham, N. D., "Wall Pressure and Shear Stress Spectra from Direct Simulations of Channel Flow," *AIAA Journal*, Vol. 44, 2006, pp. 1541–1549. doi:10.2514/1.17638

[49] Iwamoto, K., Suzuki, Y., and Kasagi, N., "Reynolds Number Effect on Wall Turbulence: Toward Effective Feedback Control," *International Journal of Heat & Fluid Flow*, Vol. 23, 2002, pp. 678–689. doi:10.1016/S0142-727X(02)00164-9

[50] Laadhari, F., "On the Evolution of Maximum Turbulent Kinetic Energy Production in a Channel Flow," *Physics of Fluids*, Vol. 14, 2002, pp. L65–L68. doi:10.1063/1.1511731

[51] Moser, R. D., Kim, J., and Mansour, N. N., "Direct Numerical Simulation of Turbulent Channel Flow up to $Re_\tau = 590$," *Physics of Fluids*, Vol. 11, 1999, pp. 943–945. doi:10.1063/1.869966

[52] Tsukahara, T., Seki, Y., Kawamura, H., and Tochio, D., "DNS of Turbulent Channel Flow at Very Low Reynolds Numbers," *Proceedings of the Fourth International Symposium on Turbulence and Shear Flow Phenomena*, 2005, pp. 935–940.

[53] Wu, X., and Moin, P., "A Direct Numerical Simulation Study on the Mean Velocity Characteristics in Turbulent Pipe Flow," *Journal of Fluid Mechanics*, Vol. 608, 2008, pp. 81–112. doi:10.1017/S0022112008002085

A. Tumin
Associate Editor